

Near surface westerly wind jet in the Atlantic ITCZ

Semyon A. Grodsky, James A. Carton, and Sumant Nigam

May 30, 2003

Revised July 1, 2003

Submitted to Geophysical Research Letters

Department of Meteorology
University of Maryland
College Park, MD 20742

senya@atmos.umd.edu

Abstract. A suite of satellite data including the QuikSCAT scatterometer winds, Tropical Rainfall Measuring Mission precipitation, TOPEX/POSEIDON sea surface height, and sea surface temperature are used to study the near surface westerly winds developing during peak months (July-September) of the West African monsoon in the Atlantic Intertropical Convergence Zone. These new data show that the westerlies appear in the form of a westerly jet. During peak years the daily near-surface westerly wind speed may exceed 10 ms^{-1} . The amplitude of the jet displays substantial decadal and interannual variability that corresponds to rainfall in West African Sahel and the frequency of African Easterly Waves. Observations and ocean model simulations show that the jet acts to cool SST through entrainment and latent heat loss and to intensify the North Equatorial Countercurrent by increasing the southward oceanic pressure gradient.

1. Introduction.

Atmospheric circulation over West Africa during the boreal summer is strongly affected by the development of a pressure trough in the lower atmosphere over the Sahara. This Sahara pressure trough contrasts with the relatively higher pressure over the Gulf of Guinea and Sahel. The resulting mostly meridional pressure gradient drives shallow westerly monsoon flow in northern summer [Carlson, 1969]. Field studies during the Global Atmospheric Research Program Atlantic Tropical Experiment (GATE) showed these shallow westerly winds are contained inside the frictional boundary layer (depth of $\sim 2\text{km}$) and within the latitude band between 0° to 20°N . They attain maximum speeds of 5 m/s at around 8°N [Reed *et al.*, 1977]. The GATE observations were taken over continental as well as ocean areas in the longitude band ranging from 31°W to 10°E ,

indicating that these shallow westerly winds occur over vast areas of the tropical Atlantic sector and thus may influence the ocean.

In this study we exploit the improved spatial and temporal resolution of newly available satellite data to provide further details on the shallow westerly winds in the latitude band of the Intertropical Convergence Zone (ITCZ). We then examine the impact of these westerlies on the surrounding ocean using observations and numerical simulations.

2. Data

This study is based on joint examination of satellite winds, rainfall, sea surface temperature (SST), sea surface height, surface drifter currents, and reanalysis winds and pressure. Satellite winds have been measured by the SeaWinds scatterometer aboard the QuikSCAT satellite [*Graf et al.*, 1998]. The SeaWinds radar has a continuous 1800 km swath and covers 93% of the ocean each day. The wind estimates have an accuracy of 2 ms^{-1} and 17° - 20° . The winds have been obtained from the QuikSCAT web site at the Jet Propulsion Laboratory/NASA where they are available optimally interpolated onto a regular $0.5^{\circ}\times 0.5^{\circ}$ -12 hr grid. Rainfall is based on a combination of the TRMM Microwave Imager, and the Precipitation Radar aboard the US/Japanese Tropical Rainfall Measuring Mission (TRMM) satellite [see *Kummerow et al.*, 2000 and citations there]. The data are the TRMM 3G68 gridded rainfall products available daily on a $0.5^{\circ}\times 0.5^{\circ}$ grid. SST has been obtained from the *Reynolds and Smith* [1994] blended satellite - in situ analysis available monthly on a $1^{\circ}\times 1^{\circ}$ grid. Sea surface height has been obtained from the TOPEX/POSEIDON altimetry Pathfinder archive (*Koblinsky*, personal communication,

1997). Winds at fixed pressure levels and sea level pressure are provided by the National Centers for Environmental Prediction/National Center for Atmospheric Research (NCEP/NCAR) reanalysis of *Kalnay et al.* [1996]. Ocean near surface drifter currents are provided by the GOOS Center at the Atlantic Oceanographic and Meteorological Laboratory/NOAA.

3. Results

During boreal summer intense surface heating over the Sahara is associated with a decrease in atmospheric pressure. The resulting meridional gradient in surface pressure turns both northern and southern trade wind systems towards the continent, resulting in the West African monsoon. Westerly winds appear most strongly where the two trade wind systems converge. A daily snapshot in **Fig. 1a** shows a westerly wind jet exceeding 15 ms^{-1} at some locations and extending across the whole basin. Westerly winds appear beginning in May and persist through September (see **Fig. 1b**) with their latitudinal position following the meridional migration of the ITCZ. They are also subject to substantial quasi-biweekly oscillations previously noted by *Janicot and Sultan* [2001] and *Grodsky and Carton* [2001].

In addition to strong seasonal and intraseasonal variability, the westerlies are subject to significant year-to-year changes as well with stronger westerlies in the summer of 1999 than 2000 (**Fig. 2**). The change in winds between these two summers is reflected in the westward extension of the Sahara pressure trough over the ocean. A simple linear three-term momentum balance relating pressure gradients, Rayleigh friction, and the Coriolis term has been used previously to describe steady motion over the tropical oceans

[Deser, 1993; Chung *et al.*, 2002]. We find that it provides a reasonable description of zonal winds associated with the westerly jet as well (using a zonal/meridional Rayleigh friction coefficients $10^{-5} \text{ s}^{-1} / 2 \times 10^{-5} \text{ s}^{-1}$ as suggested by Chiang and Zebiak [2000]) (**Fig. 1c**) to within the uncertainties in the pressure and wind estimates.

Next we consider the observed year-to-year variability through an Empirical Orthogonal Function analysis of the NCEP/NCAR reanalysis late-boreal-summer zonal winds over the central tropical Atlantic (**Fig. 3a**). This analysis shows that the westerly wind jet is the near surface expression of westerly winds that reach their maximum at ~ 700 mb [see also Reed *et al.*, 1977]. During years with stronger near-surface westerly winds stronger zonal wind shear develops in the lower troposphere that favors the development of African Easterly Waves. This relationship is demonstrated in **Fig. 3b** by comparing zonal winds with the African Easterly Wave index of Thorncroft and Huges [2001]. Since the African Easterly Waves are occasionally predecessors of tropical storms and hurricanes of the western Atlantic [Carlson, 1969], the decadal variation of the westerly wind amplitude (shown in **Fig. 3b**) corresponds to the decadal variation of Atlantic hurricane activity including the decrease between 1950s through 1980s and the increase during the 1990s.

The monsoon winds bring humid maritime air and thus rainfall to the Sahel. This relationship was demonstrated by Grist and Nicholson [2001] who have found stronger low-level westerly winds during the “wet” years in the Western Sahel (and vice-versa). Similarly, Jury *et al.* [2002] have found a relationship between zonal winds in the central Atlantic (10°S - 5°N , 40°W - 0°E) and African Rainfall. Our data in **Fig. 3b** also suggest a substantial relationship between the amplitude of the westerly wind jet and the Western

Sahel Rainfall Index of *Lamb* [1983; and personal communication, 2002]. The relationship improves after the 1960s, possibly because of improvements in the observing system.

Next we consider how the ocean responds to the westerly wind jet. The near surface westerly wind jet causes enhanced positive wind curl to the north and negative curl to the south leading to corresponding anomalies of Ekman pumping. To evaluate the importance of this effect, we examine the difference in Ekman pumping (computed from scatterometer winds), sea surface height, SST, and surface currents (**Fig.4**) between August 1999 and August 2000 (years of strong and weak westerly winds, respectively). Upward Ekman pumping velocity, w_e , along 10°N (**Fig. 4a**) was stronger during 1999 by at least 0.25 m day^{-1} . This strengthening results in thermocline shallowing and a corresponding drop in sea surface height of at least -3 cm (**Fig. 4b**). The change in the meridional difference in sea surface height across the latitude of the ITCZ is at least $\delta\eta=6 \text{ cm}$. This change also intensifies the North Equatorial Countercurrent that flows eastward following isolines of sea surface height. If we assume a mixed layer depth of $h\sim 70 \text{ m}$ at 5°N [following *White*, 1995], then a sea surface height anomaly of 6 cm distributed between the equator and 10°N increases the eastward geostrophic transport by $gf^{-1}\delta\eta h=3.2\times 10^6 \text{ m}^3\text{s}^{-1} = 3.2 \text{ Sv}$ or $\sim 15\%$ of the total North Equatorial Countercurrent transport [*Katz*, 1993]. Surface drifter currents in **Fig. 4d** are also consistent with a strengthened North Equatorial Countercurrent in August 1999 relative to August 2000.

Monthly mean wind velocity in August 1999 relative to August 2000 displays significant eastward difference of $\sim 5\text{ms}^{-1}$ in magnitude (**Fig. 4e**) due to the intense westerly wind jet in 1999. Because of the change in direction the difference in speed is $\sim 2 \text{ ms}^{-1}$. If we assume that the

mixed layer temperature anomaly is due to entrainment and latent cooling only, the anomaly ocean mixed layer temperature budget simplifies to

$$h \frac{d\delta\text{SST}}{dt} = -w_e \Delta T - \frac{a \delta W}{C_p \rho} \quad (1)$$

where $h \sim 40$ m at this latitude (10°N), the temperature discontinuity at the base of the mixed layer $\Delta T \sim 0.75$ °C [following *Swenson and Hansen, 1999*], and the linearized latent heat flux resulting from a wind speed change (δW) is $a = 6.5$ Jm⁻³ (assuming SST=28 °C and $q=90\%$). Integrating (1) over a month (the characteristic timescale of these anomalies) for $w_e \sim 0.3$ m day⁻¹ gives the entrainment contribution to SST cooling of -0.15 °C and the latent heat flux contribution -0.2 °C for $\delta W = 2$ ms⁻¹. The total SST cooling due to both mechanisms of ~ -0.3 °C is consistent with observed cooling of SST (**Fig. 4c**).

To further explore the ocean's response to anomalous winds we turn to a general circulation model configured for the tropical Atlantic. The model, based on the Geophysical Fluid Dynamics Laboratory/NOAA Modular Ocean Model (version 2) physics (see *Carton et al., 1996* for model details and simulations of interannual SST variability), has meridional boundary conditions provided by climatological seasonal sponge layers at 30°S and 50°N . The model is forced by QuikSCAT winds and a surface temperature boundary condition relaxing toward the year 2000 observed SST (with a 50-day relaxation time-scale). The control simulation consists of forcing the model with year 2000 winds (weak westerly) repeatedly for five years beginning from climatological temperature and salinity conditions. The experiment consists of modifying the winds during July-September of the sixth year by adding the 1999 minus 2000 wind differences (strong westerly) in the ITCZ belt bounded by a Gaussian filter centered at 30°W , 9°N with 30° longitude and 3° latitude spatial scales (see **Fig. 5a**). The spatial and temporal

bounding of the wind difference eliminates the Atlantic Niño warming (like that in **Fig 4c**, see *Carton et al.*, 1996 for further details) and concentrates our attention on the dynamical effect of the westerly wind jet upon the ocean. The experiment is compared with the fifth year of the control simulation.

In general agreement with observations, the experiment shows stronger upward pumping to the north and stronger downward pumping to the south of the westerly wind jet that results in an increase in the meridional gradient of sea surface height (**Fig. 5b**) and a strengthening of the North Equatorial Countercurrent. There are several areas of disagreement between the observations and experiment as well. The simulated increase of the zonal current ($\sim 10 \text{ cm s}^{-1}$, **Fig. 5d**) is roughly half that observed by the drifters ($\sim 20 \text{ cm s}^{-1}$, **Fig. 4d**). The simulated current has a southward component that is not observed. The simulated SST decrease $\sim -0.6 \text{ }^\circ\text{C}$ (**Fig. 5c**) is stronger than the $\sim 0.3 \text{ }^\circ\text{C}$ observed (**Fig. 4c**) because of the increase in southward current.

4. Discussion and conclusion

Examination of daily surface winds provided by the scatterometer onboard the QuikSCAT satellite indicates that a strong westerly wind jet develops in the Atlantic ITCZ. The monthly mean wind speed in this jet during late boreal summer could exceed 7 ms^{-1} . During this time it extends well into the central basin between 40°W and the African coast. The jet also shows strong intraseasonal variability. During peak years the daily near surface westerly wind speed may exceed 10 ms^{-1} .

Exploration of the impact of the westerly wind jet on the ocean shows that it strengthens the meridional gradient of Ekman pumping. This causes cooling of the mixed

layer and shallowing of the thermocline to the north and warming of the mixed layer and deepening of the thermocline to the south. The associated changes in the meridional gradient of sea surface height could intensify the eastward North Equatorial Counter Current transport by around 15%. Intensification of the winds also causes an increase in latent heat loss. We compare the Ekman pumping and latent heat loss effects during 2000 relative to 1999 and find they have similar impact on reducing SST.

The westerly wind jet is geostrophically related to the southwestward extension of the Sahara pressure trough. The westerly jet is in near-geostrophic balance with the meridional atmospheric pressure gradient set up by the Sahara trough extension. This relationship leaves us with the question of what mechanisms regulate the southward extension of the Sahara trough over the ocean and its year-to-year variation. *Tomas and Webster* [1997] have argued that the near surface westerly jet could result from the clockwise turning of the southern trades after their entry into the northern latitudes if a southward cross-equatorial pressure gradient exists. By considering the nonlinear vorticity balance, they have found that the low-level westerlies should increase north of the zero absolute vorticity line. But this mechanism doesn't explain what cause the extension in the Sahara trough and the southward pressure gradient. A more complete examination of this question will likely require a fully coupled model.

Acknowledgments.

This work was supported by NOAA's office of Oceanic and Atmospheric Research and Office of Global Programs and by the National Science Foundation. We appreciate comments from Peter Lamb who also has provided an update of the West

Sahel Rainfall Index. We are grateful to Xianhe Cao for assistance in running the ocean model. Drifter data has been obtained from the Drifter DAC of the GOOS Center at NOAA/AOML. Quikscat wind has been obtained from the NASA/NOAA sponsored system Seaflux at JPL through the courtesy of W. Timothy Liu and Wenqing Tang. Comments and suggestions of anonymous reviewers were useful and stimulating.

References.

- Carlson, T.N., Synoptic histories of three African disturbances that developed into Atlantic hurricanes, *Mon. Wea. Rev.*, 97, 256-276, 1969.
- Carton, J.A., X.H. Cao, B.S. Giese, and A.M. daSilva, Decadal and interannual SST variability in the tropical Atlantic Ocean, *J. Phys. Oceanogr.*, 26 (7), 1165-1175, 1996.
- Chiang, J.C.H, S.E. Zebiak, and M.A. Cane, Relative roles of elevated heating and surface temperature gradients in driving anomalous surface winds over tropical oceans, *J. Atmos. Sci.*, 58, 1371-1394, 2001
- Chung, C., S. Nigam, and J.A. Carton, SST-forced surface wind variability in the tropical Atlantic: An empirical model, *J. Geoph. Res.*, 107(D15), doi: 10.129/2001JD000324, 2002.
- Deser, C., Diagnosis of the surface momentum balance over the tropical Pacific ocean, *J. Clim.*, 6, 64-74, 1993.
- Graf, J., C. Sasaki, C. Winn, W.T. Liu, W. Tsai, M. Freilich, and D. Long, NASA Scatterometer Experiment., *Acta Astronautica*, 43, 397-407, 1998.
- Grist, J.P., and S.E. Nicholson, A study of the dynamics factors influencing the rainfall variability in the West African Sahel, *J. Clim.*, 14, 1337-1359, 2001.
- Grodsky, S.A., and J.A. Carton, Coupled land/atmosphere interactions in the West African Monsoon, *Geoph. Res. Let.*, 28, 1503-1506, 2001.
- Janicot, S., and B. Sultan, Intra-seasonal modulation of convection in the West African monsoon, *Geoph. Res. Let.*, 28, 523-526, 2001.

- Jury, M.R., D.B. Enfield, and J-L Melice, Tropical monsoon around Africa: Stability of ENSO associations and links with continental climate, *J. Geoph. Res.*, 107(C10), 3151, doi: 10.129/2000JC000507, 2002.
- Kalnay, E., and Coauthors, The NCEP/NCAR 40-year reanalysis project, *Bull. Amer. Meteorol. Soc.*, 77, 437-471, 1996.
- Katz, E.J., An interannual study of the Atlantic North Equatorial Countercurrent, *J. Phys. Oceanogr.*, 23, 116-123, 1993.
- Kummerow, C., and Coauthors, The Status of the Tropical Rainfall Measuring Mission (TRMM) after Two Years in Orbit. *J. Applied Meteor.*, 39, 1965-1982, 2000.
- Lamb, P. J., Sub-Saharan rainfall update for 1982: Continued drought, *J. Climatol.*, 3, 419-422, 1983.
- Reed, R. J., D. C. Norquist, and E.E. Recker, The structure and properties of African disturbances as observed during phase III of GATE, *Mon. Wea. Rev.*, 105, 317-333, 1977.
- Reynolds, R. W., and T. M. Smith, Improved global sea surface temperature analyses using optimum interpolation, *J. Clim.*, 7, 929-948, 1994.
- Swenson, M. S., and D. V. Hansen, Tropical Pacific ocean mixed layer heat budget: The Pacific Cold Tongue, *J. Phys. Oceanogr.*, 29, 69-81, 1999.
- Thorncroft, C., and K. Hodges, African easterly wave variability and its relationship to Atlantic tropical cyclone activity, *J. Clim.*, 14, 1166-1179, 2001.
- Tomas, R. A., and P. J. Webster, The role of internal variability in determining the location and strength of near-equatorial convection, *Quart. J. Roy. Meteor. Soc.*, 123, 1445-1482, 1997.
- White, W. B., Design of a global observing system for gyre-scale upper ocean temperature variability, *Progress in Oceanogr.*, 36, Pergamon, 169-217, 1995.

Figure legends.

Fig.1 (a) QuikSCAT winds on 17 August 1999 and the NCEP/NCAR mean sea surface height pressure. (b) Observed (solid) and calculated (symbols) zonal wind averaged 25°W - 15°W. (c) Latitude-time diagram of the QuikSCAT daily zonal winds averaged 25°W - 15°W. The latitude of the strongest wind convergence is shown as a proxy for the ITCZ position. Only the eastward zonal wind velocity isolines are drawn at [2.5, 5, 7.5, 10, 12.5] ms⁻¹. Zonal wind exceeding 5 ms⁻¹ is shaded. Vertical lines show the beginning and end of each August.

Fig.2. August mean QuikSCAT winds, NCEP/NCAR reanalysis mean sea surface height pressure, and TRMM rainfall in (a) 1999 and (b) 2000. The 1013 mb and minimum pressure contour over Sahara are labeled. Pressure lower than 1013 mb is shaded. Only rainfall exceeding 0.25 mm hr⁻¹ is shown in dark gray.

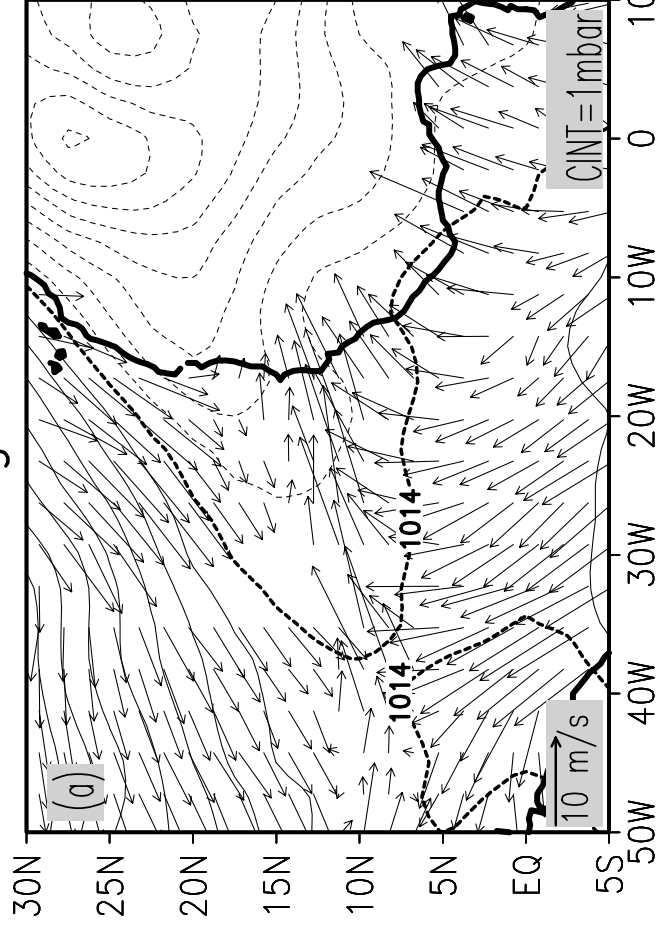
Fig.3 (a) First rotated Empirical Orthogonal Function of the August zonal winds averaged 30°W to 10°W. (b) Time series of first EOF amplitude (U), number of African Easterly Waves (*AEW*) of *Thorncroft and Huges* [2001], and the Western Sahel Rainfall Index (*WSRI*) of *Lamb* [1983].

Fig.4 1999 minus 2000 observed differences during August. (a) Ekman pumping velocity (positive - upward). (b) Sea surface height. (c) Sea surface temperature. (d) Drifter surface currents. (e) Wind velocity (arrows) and wind speed (contours). Contours are drawn at [-1.5 -0.5 0.5 1.5 2.5] ms⁻¹. Wind speed increase exceeding 0.5 ms⁻¹ contour is shaded. (f) Mean sea level pressure.

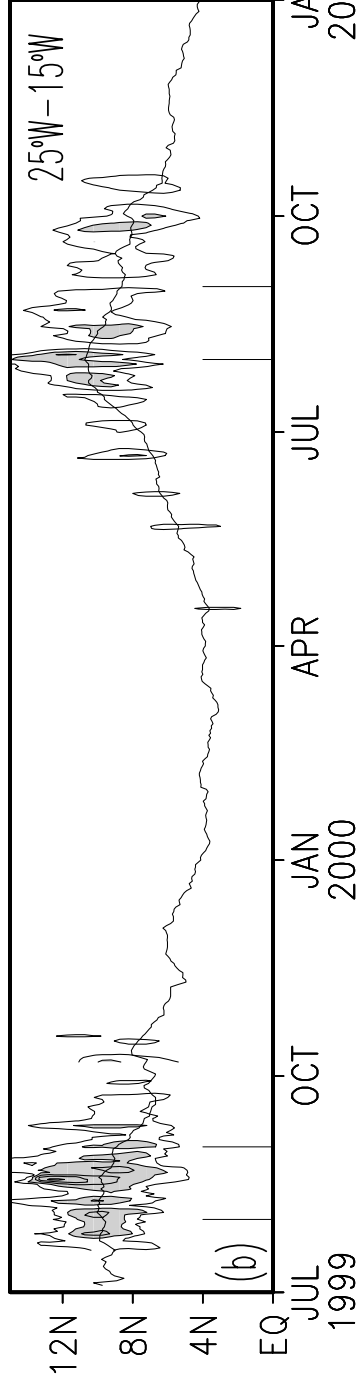
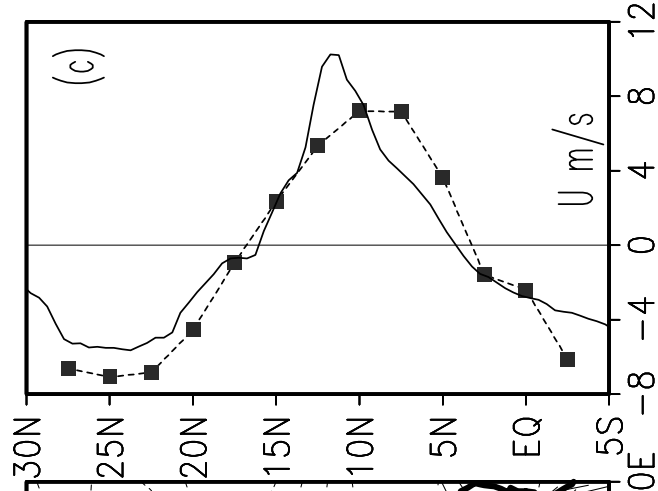
Fig.5 1999 minus 2000 simulated differences during August. (a) Wind stress (only values exceeding 0.1 dyn cm⁻² in magnitude are shown). (b) Sea surface height. (c)

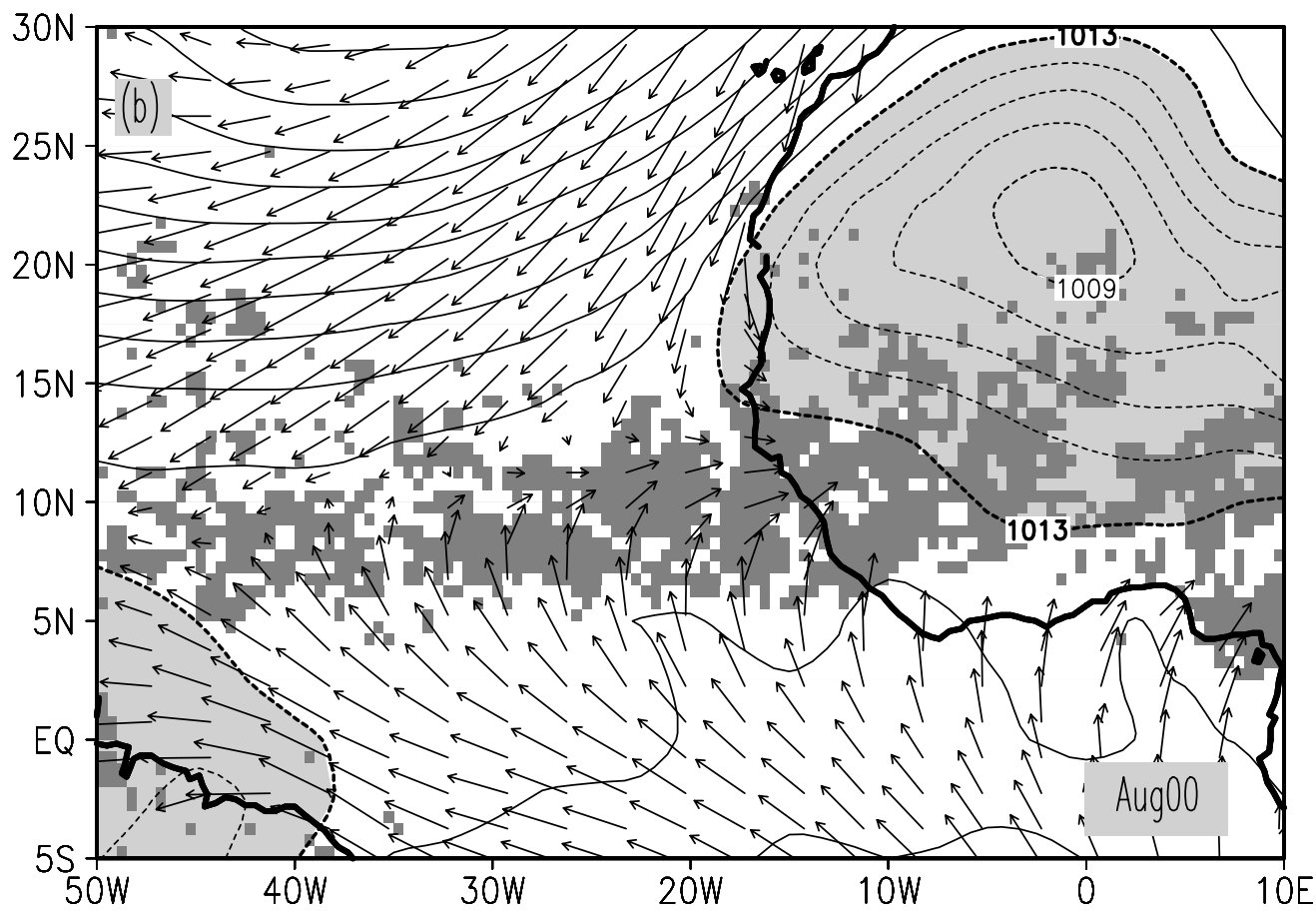
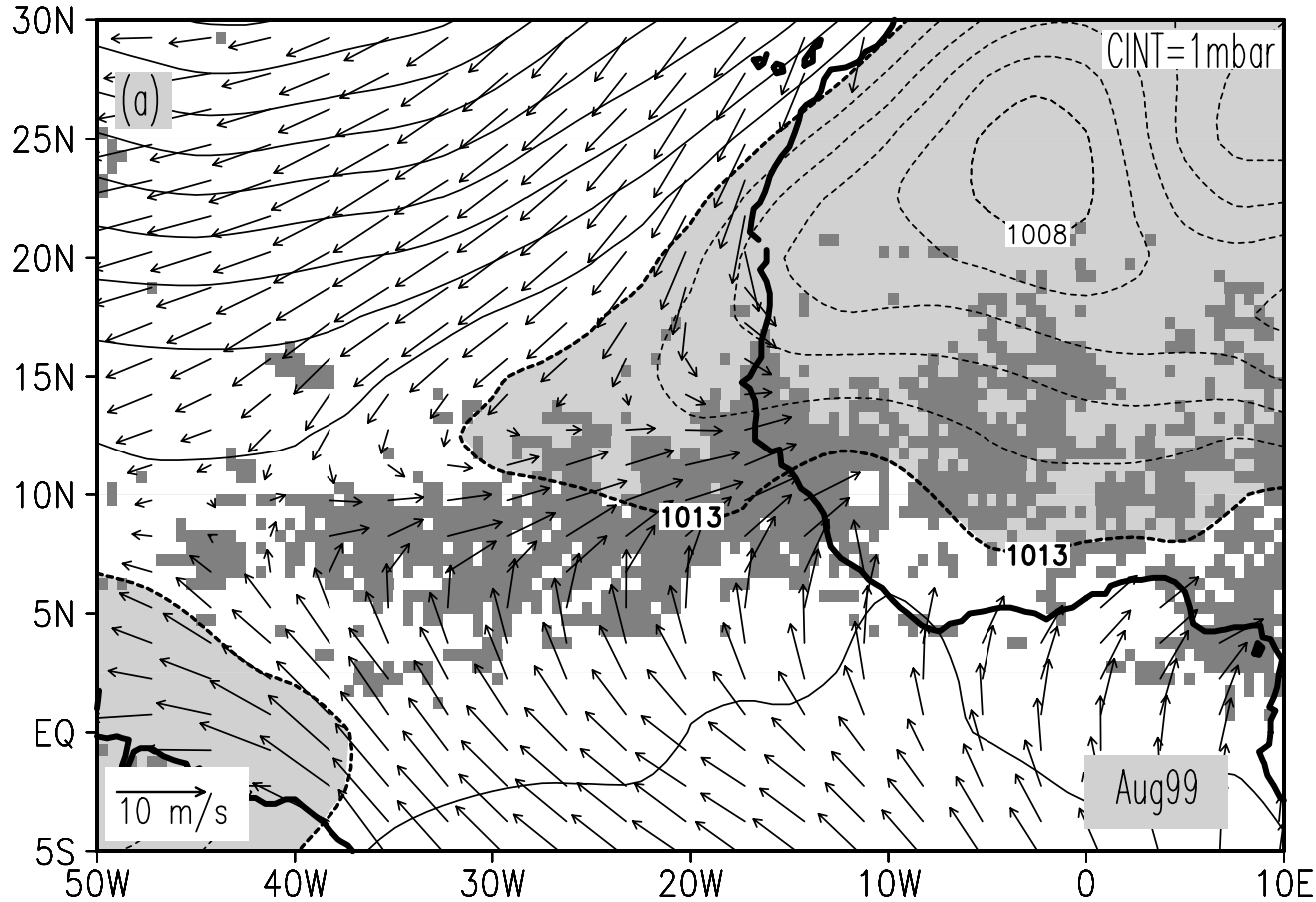
Sea surface temperature. (d) Surface currents (only values exceeding 2 cm s^{-1} in magnitude are shown).

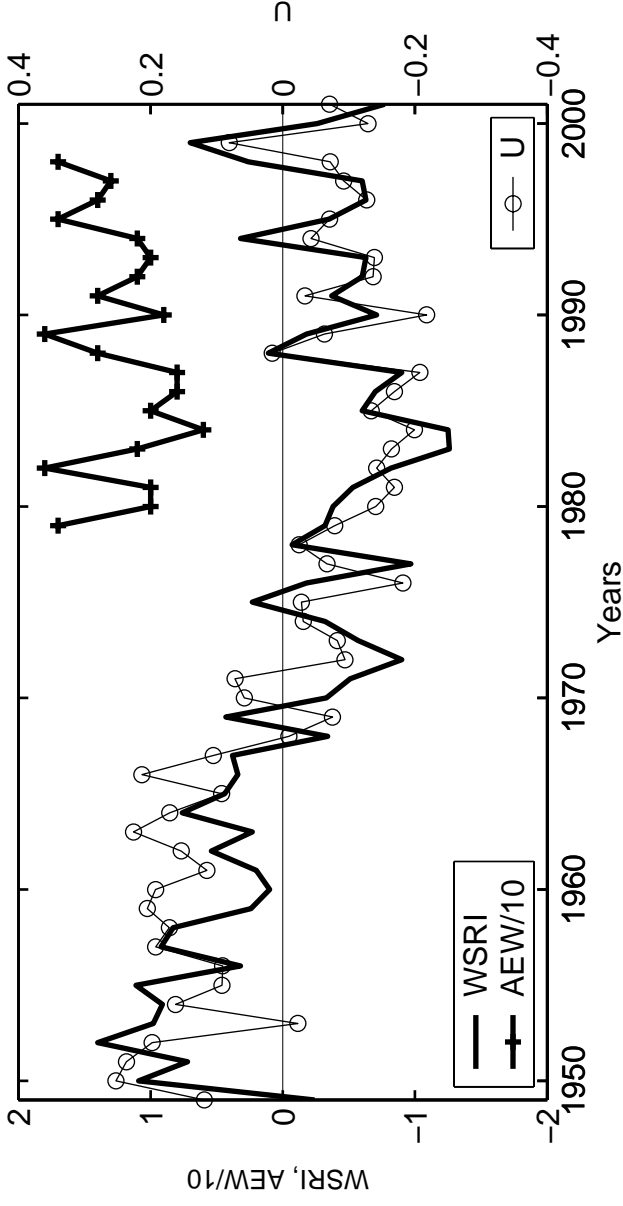
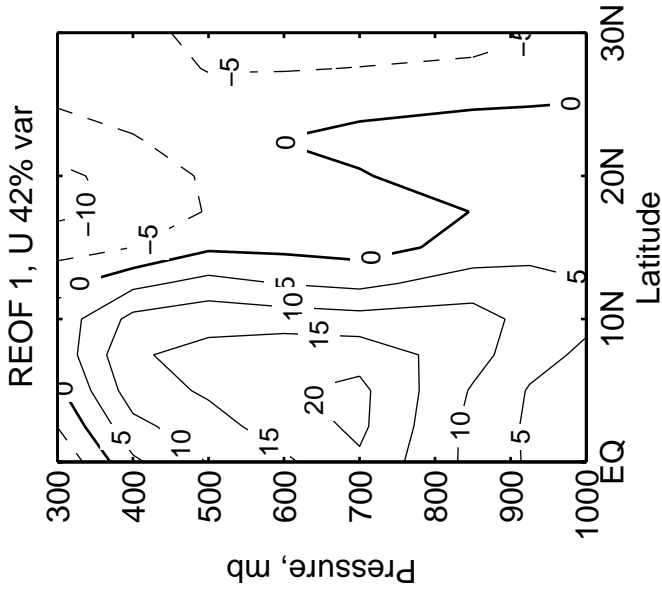
17 August 1999



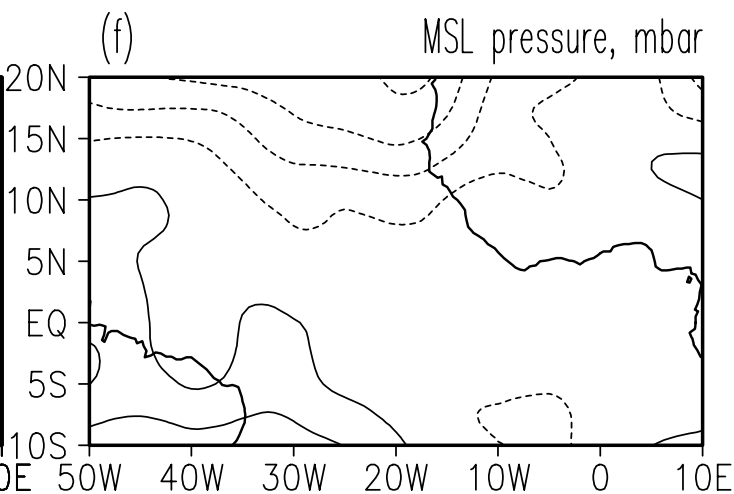
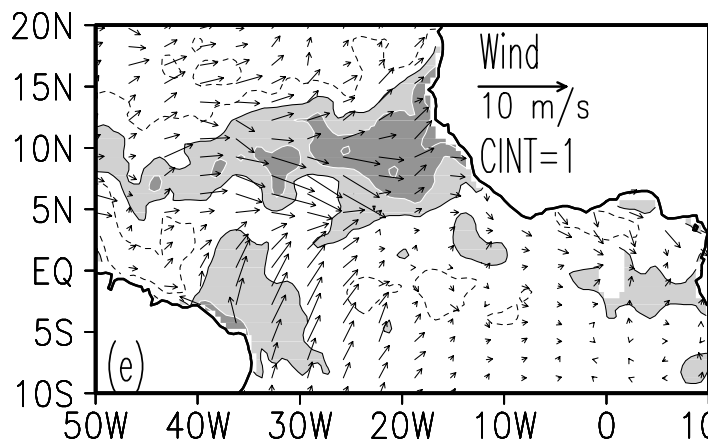
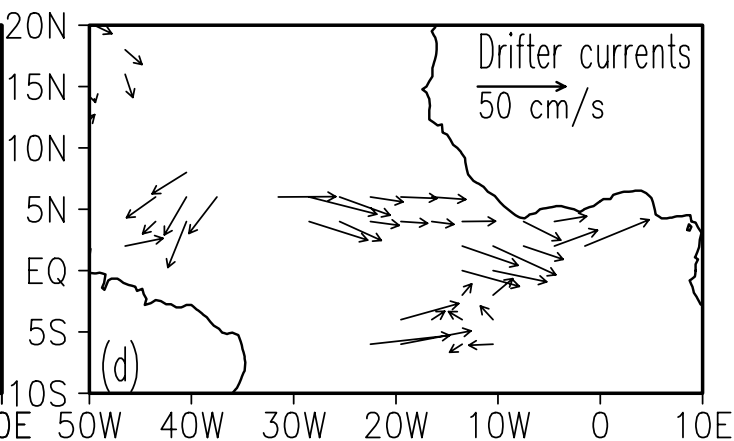
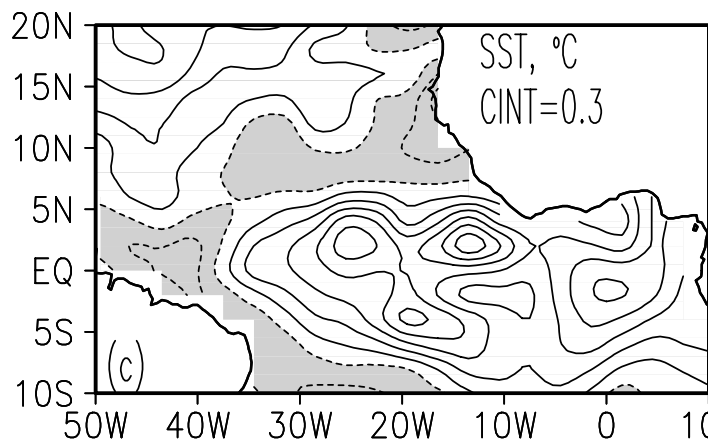
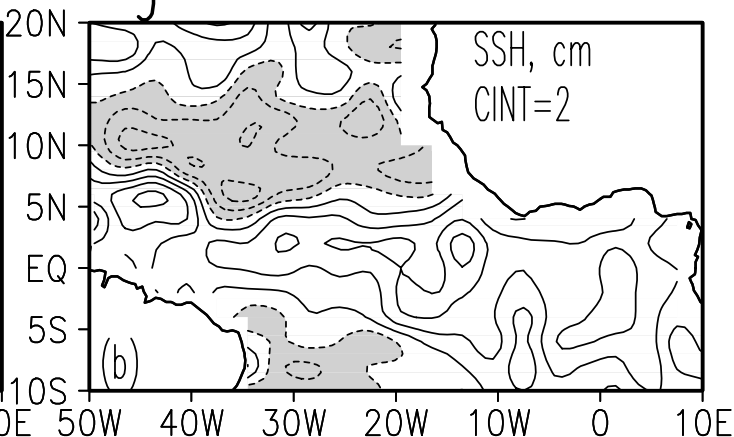
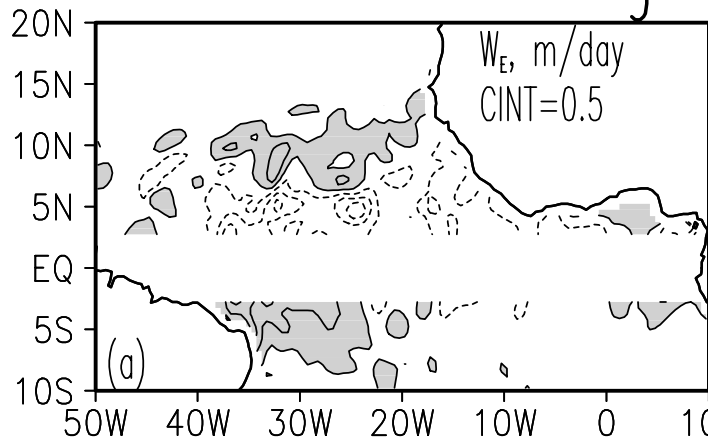
25°W – 15°W







Aug99–Aug00



Aug99 – Aug00

